A SCS CMOS MICROMIRROR FOR OPTICAL COHERENCE TOMOGRAPHIC IMAGING

Huikai Xie[1], Yingtian Pan[3, 4] and Gary K. Fedder[1, 2]
[1]Department of Electrical & Computer Engineering; [2]Robotics Institute; [3]Science and Technology Center
Carnegie Mellon University, 5000 Forbes Avenue, Pittsburgh, PA 15213
[4]Departments of Medicine and Bioengineering
University of Pittsburgh, 3550 Terrace Street, Pittsburgh, PA 15261
E-mail: xie@ece.cmu.edu; pan@andrew.cmu.edu; fedder@ece.cmu.edu

ABSTRACT

This paper reports a single-crystalline silicon (SCS) micromirror used for laser beam scanning in an endoscopic optical coherence tomography (OCT) system. The micromirror is fabricated by using a deep reactive-ion-etch (DRIE) post-CMOS micromachining process. Thin bimorph actuation structures and movable bulk silicon structures are simultaneously achieved. The micromirror is 1 mm by 1 mm in size, coated with aluminum, and thermally actuated by an integrated polysilicon heater. The radius of curvature of the mirror surface is 50 cm. The mirror rotates 17˚ when a 15 mA current is applied. Cross-sectional images of 500×1000 pixels covering an area of 2.9 mm by 2.8 mm are acquired at 5 frames/s by using an OCT system based on this micromirror.

INTRODUCTION

Numerous micromirrors have been demonstrated by using either surface- or bulk- micromachining processes [1][2]. Nevertheless, micromachined large, flat mirrors with large tunable displacement or rotation angle required by some applications such as medical imaging, interferometer systems and laser beam steering are rarely reported but are demanding more attention. For example, current endoscopic OCT devices for *in vivo* imaging of internal organs use either a rotating hollow cable carrying a single-mode optical fiber or a small galvanometric plate swinging the distal fiber tip to perform transverse scanning [3][4]. If the scanning devices can be replaced by a micromirror, endoscopic OCT systems may be more compact and potentially low cost. However, the micromirror must be flat and large to maintain high light-coupling efficiency and spatial resolution, and must have large rotation angle to meet the scanning range.

Conant *et al.* reported a ϕ550 μm SCS based micromirror for high speed scanning (34 kHz) by using silicon-on-insulator (SOI) wafers and two-side alignment [5]. Su *et al.* demonstrated a flat, 0.25 mm by 0.25 mm mirror by assembling an SCS mirror on top of polysilicon actuators [6]. However, using high voltage to achieve large rotation angle is still a problem for interior body applications.

In prior research, multilayer metal/silicon oxide beams have included an embedded polysilicon heater to tune the resonant frequency of a gyroscope's drive mode [7]. Similar to the thermally actuated micromirror reported in [8], the beams bend down when a current is applied to the polysilicon heater. Using the same concept and combining a deep reactive-ion-etch (DRIE) CMOS-MEMS process [9], we have developed a bulk-Si mirror actuated electro-thermally to a large rotation angle. The operational principle and mirror design are introduced first, followed by the detailed fabrication procedure, the characterization results of the mirror flatness and laser scanning static response, and application of the micromirror to an OCT system.

MIRROR DESIGN

The schematic of the mirror design is shown in Fig. 1. The mirror is attached to a bi-layer aluminum/silicon dioxide mesh with polysilicon encapsulated within the silicon dioxide to form a bimorph

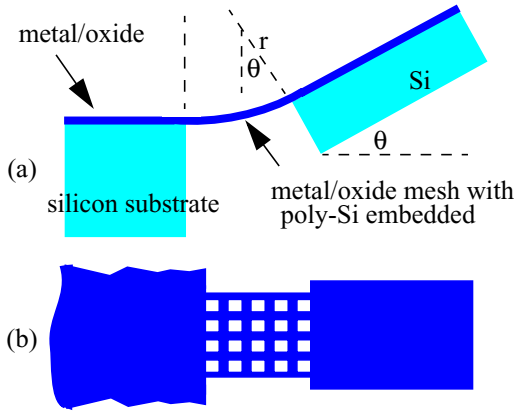

Figure 1. The mirror conceptual design. (a). Cross-sectional view; and (b) top view.

thermal actuator. The mesh curls up after being released due to the tensile stress in the aluminum layer and compressive residual stress in the bottom silicon dioxide layer. Therefore, the radius of curvature of a bimorph beam is determined by both the initial curling and the temperature change from the polysilicon heating, and is given by $\frac{1}{r} = \frac{1}{R_0} - \frac{1}{r_T}$, where r is the actual radius of curvature, R_0 is the initial radius of curvature and r_T is the radius of curvature due to the temperature change. By ignoring the thin polysilicon layer, r_T is readily derived as[11]

$$r_T = \frac{2}{3} \cdot \frac{t_1^2 + t_2^2 + \frac{3}{2} t_1 t_2 + \frac{1}{4}\left(\frac{E_1 t_1^3}{E_2 t_2} + \frac{E_2 t_2^3}{E_1 t_1}\right)}{\Delta T(\alpha_1 - \alpha_2)(t_1 - t_2)}$$

where t_i, E_i and α_i are the thickness, Young's modulus and thermal expansion coefficients of the metal layer (i=1) and the oxide layer (i=2), and ΔT is the temperature change on the beam. R_0 is a fixed value for a given process. For instance, the radius of curvature of micromechanical beams made of metal1/ oxide layers in the Agilent 0.5 µm 3-metal CMOS process was measured to be 290 µm [10].

A bulk silicon mirror coated with metal and dielectrics is attached at the end of the mesh. The tilt of the mirror follows the curvature of the mesh, and is given by $\theta = \frac{L}{r}$, where L is the length of the mesh. The choice of L depends on the requirements to speed and power consumption, and rigidity of the mirror assembly.

FABRICATION

The micromirror is fabricated with a DRIE CMOS-MEMS process [9]. We start with a deep anisotropic backside etch leaving a 10 µm to 100 µm-thick SCS membrane with thickness dependent on etch time (Fig. 2 (a)). This thick SCS membrane is used as the mechanical support of the mirror to keep the mirror flat. The cavity formed by the backside etch leaves ample space for large actuation range. Next, an anisotropic dielectric etch is performed from the front side (Fig. 2 (b)), followed by a directional silicon etch (Fig. 2 (c)). Finally, an isotropic Si etch is performed to undercut the silicon underneath the mesh (Fig. 2(d)). The mesh is 1.8 µm thick and thus flexible in the z-direction (out-of-plane).

This process is maskless, only uses dry etch steps, is completely compatible with commercial CMOS processes and has no release sticking problems. Fig. 3(a) shows a scanning electron micrograph (SEM) of a fabricated micromirror. The mirror tilts 17˚ at room temperature. Fig. 3(c) is a close-up of one cor-

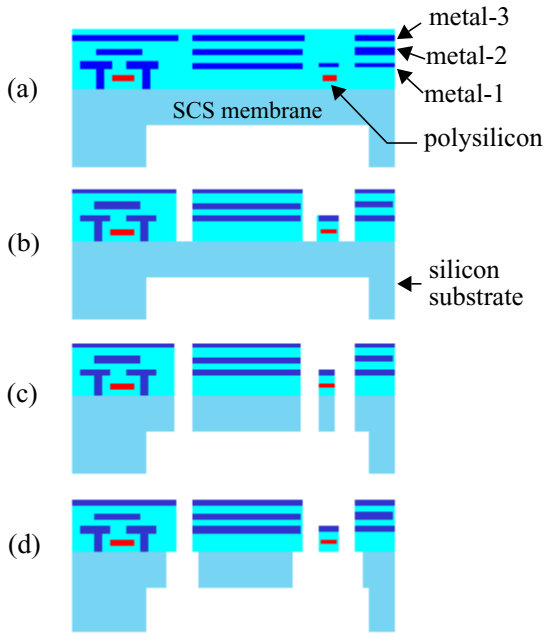

Figure 2. DRIE CMOS-MEMS process flow: (a) backside etch; (b) oxide etch; (c) deep Si etch; and (d) Si undercut.

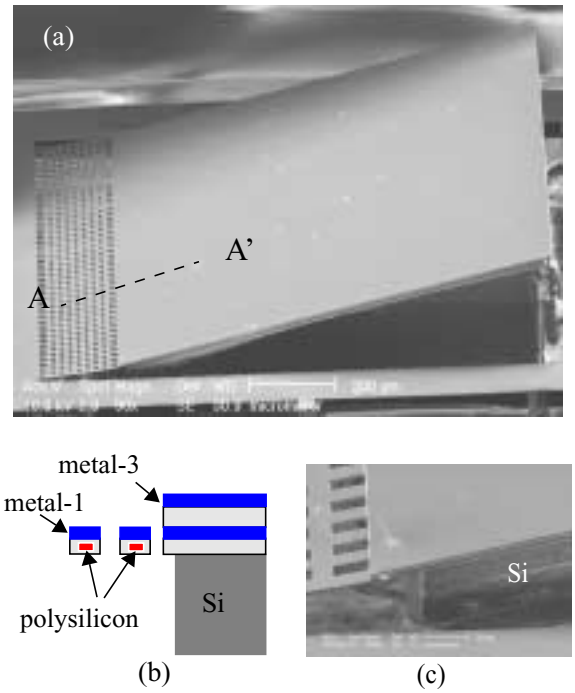

Figure 3. SEMs of a released mirror: (a) side view; (b) cross-section of A-A'; and (c) close-up of one corner.

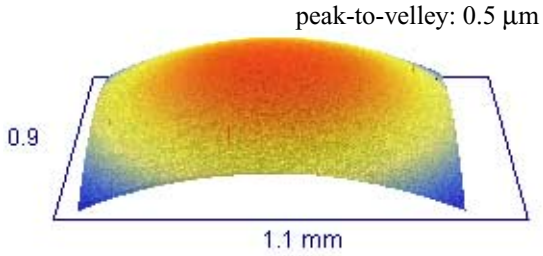

Figure 4. Surface profile of the micromirror

ner of the mirror showing the supporting 40 µm-thick bulk silicon underneath the mirror Al surface.

CHARACTERIZATION

The structural SCS layer backing the mirror provides very good flatness across the 1 mm surface. Fig. 4 shows the surface profile of the active mirror area measured by using a Wyko optical profilometer. The peak-to-valley deflection is 0.5 µm, which converts to a radius of curvature of 50 cm. The mirror can be even flatter if the SCS membrane is made thicker during the backside etch step (Fig. 2(a)).

Fig. 5 shows the measured rotation angle at different heater currents. The hysteretic behavior of the angle as a function of current is believed to be from mechanical non-linearity in the mesh structure. The resistance of the heater is 2.2 kΩ. The maximum current the polysilicon heater can carry before thermal damage occurs at 18 mA. One mirror has been continuously working at a 2 Hz scan rate for more than half a year. No significant degradation or aging is observed. The resonant frequency of the mirror is 165 Hz, which meets the scanning speed requirement for most endoscopic applications.

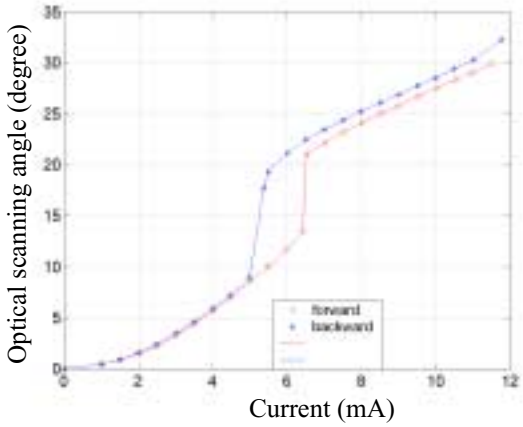

Figure 5. Optical scanning angle versus applied current.

OCT APPLICATION

Fig. 6 illustrates a 5 mm diameter endoscopic OCT system equipped with the above micromirror [12]. A broadband light source is guided equally into two single-mode fibers through a beam splitter to form a Michelson interferometer. The light in the sample arm is collimated by an fiber-optic aspherical lens (CM), deflected by a conventional mirror and the beam steering micromirror. It is then focused on the detecting biological sample, which reflects part of the incident light back to the sample arm. The light in the reference arm is linearly scanned in the axial direction by an optical delay line. Because broadband light has short temporal coherence, this will permit detection of backscattering from different depth within the biological sample. Fig. 7 is an OCT image of a porcine urinary bladder *in vivo* (through cystotomy), demonstrating that the endoscopic OCT system using a MEMS micromirror can delineate the morphology of the bladder at high resolution. Since the scanning is operated by the micromirror inside the endoscope, no mechanical movement of

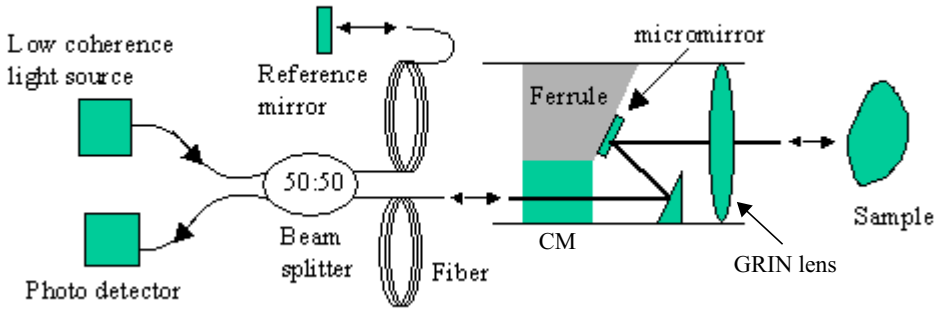

Figure 6. Schematic of the MEMS-based endoscopic OCT system.

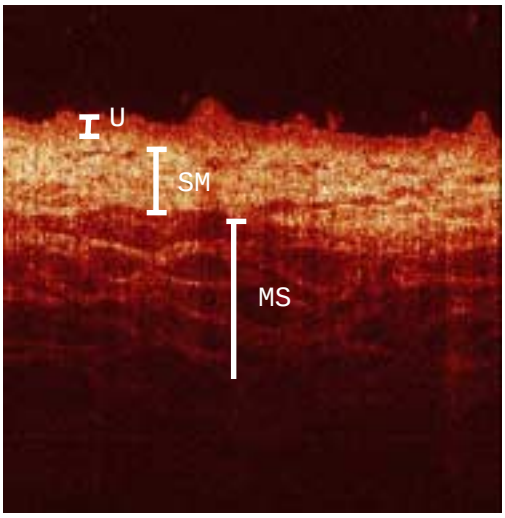

Figure 7. *In vivo* 2-D endoscopic OCT of porcine bladder through cystotomy. U: urothelium, SM: submucosa, MS: muscularis layer. Image size: 500x1000 pixels covering an area of 2.9x2.8 mm^2.

the endoscope is needed. This offers enormous advantage to the development of laser scanning endoscopes for noninvasive or minimally invasive imaging diagnosis within a wide variety of inner organs.

CONCLUSIONS

A large, flat bulk-Si CMOS-MEMS mirror was demonstrated and applied to an OCT endoscope for *in vivo* medical imaging. The fabrication process is simple and compatible with conventional CMOS processes. Rotation sensors and angular control circuits can be integrated on the same chip with the mirrors. This type of micromirror is especially suitable for laser scanning endoscopy that requires large rotation angle and low drive voltage.

ACKNOWLEDGEMENT

This work is supported in part by DARPA under the AFRL, Air Force Material Command, USAF, under agreement F30602-97-20323, NIH contract NIH-1-R01-DK059265-01, and the Whitaker Foundation contract 00-0149.

REFERENCE

[1]. L. J. Hornbeck, "Digital Light Processing and MEMS: an overview," *Digest. IEEE/LEOS 1996 Summer Topical Meetings*, Keystone, CO, USA; 5-9 Aug. 1996, p.7-8.

[2]. V.A. Aksyuk, F. Pardo, C.A. Bolle, S. Arney, C.R. Giles, D.J. Bishop, "Lucent Microstar micromirror array technology for large optical crossconnects," *Proc. SPIE - Int. Soc. Opt. Eng. (USA),* Santa Clara, CA, USA; 18-20 Sept. 2000, p320-324.

[3]. G. J. Tearney, M. E. Brezinski, B. E. Bouma, S. A. Boppart, C. Pitris, J. F. Southern, and J. G. Fujimoto, "In Vivo Endoscopic Optical Biopsy with Optical Coherence Tomography," *Science*, Vol. 276 (1997), p.2037-2039.

[4]. A. M. Sergeev *et al.*, "*In vivo* endoscopic OCT imaging of precancer and cancer states of human mucosa," *Optics Express*, Vol. 1 (1997), p.432-440.

[5]. R. Conant, J. Nee, K. Lau and R. Muller, "A flat high-frequency scanning micromirror," *Technical Digest. 2000 Solid-State Sensor & Actuator Workshop*, Hilton Head, SC, p.6-9.

[6]. G.-D. Su, H. Toshiyoshi, and M.C. Wu, "Surface-micromachined 2-D optical scanners with high-performance single-crystalline silicon micromirrors," *IEEE Photonics Technology Letters* , Vol. 13, p.606-608.

[7]. H. Xie, and G. K. Fedder., "A CMOS-MEMS lateral-axis gyroscope," *Technical Digest of the 14th IEEE International Conference on Micro Electro Mechanical Systems (MEMS 2001)*, Interlaken, Switzerland, p.162-165

[8]. J. Buhler, J. Funk, O.Paul, F.-P. Steiner, H. Baltes, *Sensors & Actuators A*, Vol. 46-47 (1995), p.572-575.

[9]. H. Xie, L. Erdmann, X. Zhu, G.K. Fedder, *Technical Digest. Solid-State Sensor and Actuator Workshop*, Hilton Head Island, SC, USA; June 4-8, 2000, p77-80.

[10]. M.S.-C. Lu, X. Zhu, and G.K. Fedder, *Symposium on Microelectromechanical Structures for Materials Research*, San Francisco, CA, April 1998, p.27-32.

[11]. J. Buhler, "Deformable Micromirror Arrays by CMOS Technology," Ph.D. Thesis, ETH Zurich, 1997.

[12]. Y. Pan, H. Xie, G.K. Fedder, to appear in *Optics Letters*, December 15, 2001.